







# NBS TECHNICAL NOTE 652

U.S. DEPARTMENT OF COMMERCE / National Bureau of Standards

## Development and Construction of an Electromagnetic Near-Field Synthesizer

QC  
100  
45753  
no. 652  
1974  
c. 2

## NATIONAL BUREAU OF STANDARDS

The National Bureau of Standards<sup>1</sup> was established by an act of Congress March 3, 1901. The Bureau's overall goal is to strengthen and advance the Nation's science and technology and facilitate their effective application for public benefit. To this end, the Bureau conducts research and provides: (1) a basis for the Nation's physical measurement system, (2) scientific and technological services for industry and government, (3) a technical basis for equity in trade, and (4) technical services to promote public safety. The Bureau consists of the Institute for Basic Standards, the Institute for Materials Research, the Institute for Applied Technology, the Institute for Computer Sciences and Technology, and the Office for Information Programs.

**THE INSTITUTE FOR BASIC STANDARDS** provides the central basis within the United States of a complete and consistent system of physical measurement; coordinates that system with measurement systems of other nations; and furnishes essential services leading to accurate and uniform physical measurements throughout the Nation's scientific community, industry, and commerce. The Institute consists of a Center for Radiation Research, an Office of Measurement Services and the following divisions:

Applied Mathematics — Electricity — Mechanics — Heat — Optical Physics — Nuclear Sciences<sup>2</sup> — Applied Radiation<sup>2</sup> — Quantum Electronics<sup>3</sup> — Electromagnetics<sup>3</sup> — Time and Frequency<sup>3</sup> — Laboratory Astrophysics<sup>3</sup> — Cryogenics<sup>3</sup>.

**THE INSTITUTE FOR MATERIALS RESEARCH** conducts materials research leading to improved methods of measurement, standards, and data on the properties of well-characterized materials needed by industry, commerce, educational institutions, and Government; provides advisory and research services to other Government agencies; and develops, produces, and distributes standard reference materials. The Institute consists of the Office of Standard Reference Materials and the following divisions:

Analytical Chemistry — Polymers — Metallurgy — Inorganic Materials — Reactor Radiation — Physical Chemistry.

**THE INSTITUTE FOR APPLIED TECHNOLOGY** provides technical services to promote the use of available technology and to facilitate technological innovation in industry and Government; cooperates with public and private organizations leading to the development of technological standards (including mandatory safety standards), codes and methods of test; and provides technical advice and services to Government agencies upon request. The Institute consists of a Center for Building Technology and the following divisions and offices:

Engineering and Product Standards — Weights and Measures — Invention and Innovation — Product Evaluation Technology — Electronic Technology — Technical Analysis — Measurement Engineering — Structures, Materials, and Life Safety<sup>4</sup> — Building Environment<sup>4</sup> — Technical Evaluation and Application<sup>4</sup> — Fire Technology.

**THE INSTITUTE FOR COMPUTER SCIENCES AND TECHNOLOGY** conducts research and provides technical services designed to aid Government agencies in improving cost effectiveness in the conduct of their programs through the selection, acquisition, and effective utilization of automatic data processing equipment; and serves as the principal focus within the executive branch for the development of Federal standards for automatic data processing equipment, techniques, and computer languages. The Institute consists of the following divisions:

Computer Services — Systems and Software — Computer Systems Engineering — Information Technology.

**THE OFFICE FOR INFORMATION PROGRAMS** promotes optimum dissemination and accessibility of scientific information generated within NBS and other agencies of the Federal Government; promotes the development of the National Standard Reference Data System and a system of information analysis centers dealing with the broader aspects of the National Measurement System; provides appropriate services to ensure that the NBS staff has optimum accessibility to the scientific information of the world. The Office consists of the following organizational units:

Office of Standard Reference Data — Office of Information Activities — Office of Technical Publications — Library — Office of International Relations.

<sup>1</sup> Headquarters and Laboratories at Gaithersburg, Maryland, unless otherwise noted; mailing address Washington, D.C. 20234.

<sup>2</sup> Part of the Center for Radiation Research.

<sup>3</sup> Located at Boulder, Colorado 80302.

<sup>4</sup> Part of the Center for Building Technology.

1. 1974  
acc.  
00  
753  
652  
74  
2

# Development and Construction of an Electromagnetic Near-Field Synthesizer

Frank M. Greene

Electromagnetics Division  
Institute for Basic Standards  
U.S. National Bureau of Standards  
Boulder, Colorado 80302

t. Technical note no. 652



---

U.S. DEPARTMENT OF COMMERCE, Frederick B. Dent, Secretary

NATIONAL BUREAU OF STANDARDS, Richard W. Roberts, Director

Issued May 1974

**National Bureau of Standards Technical Note 652**

**Nat. Bur. Stand. (U.S.), Tech. Note 652, 44 pages (May 1974)**

**CODEN: NBTNAE**

## CONTENTS

	<u>Page</u>
1. INTRODUCTION-----	2
2. THE RF MAGNETIC-FIELD GENERATOR-----	3
2.1 The Physical Characteristics of the Loop Inductor--	3
2.2 The Electrical Characteristics of the Loop Inductor--	4
2.3 The Loop-Inductor Matching Networks-----	9
2.4 The Vacuum Variable Tuning Capacitors-----	11
2.5 The Balun Transformer-----	11
2.6 The Water Cooling of the Inductor-----	12
3. THE RF ELECTRIC-FIELD GENERATOR-----	15
3.1 The Physical Characteristics of the Parallel-Plate Strip Line-----	15
3.2 The Parallel-Plate Matching Network-----	16
3.3 The Electrical Characteristics of the Parallel-Plate Strip Line-----	19
4. THE COMPLETE SYNTHESIZER UNIT-----	19
4.1 A General Description-----	19
4.2 The Effect of the Shielded Room-----	20
4.3 The RF Excitation of the Field Generators-----	21
4.4 The Phase-Shift Networks-----	21
4.5 The RF Exposure Capability-----	23
5. SUMMARY AND CONCLUSIONS-----	24
6. ACKNOWLEDGMENT-----	26
 <u>APPENDIX A</u>	
7. THE ELECTRIC FIELD ASSOCIATED WITH A LOOP INDUCTOR-----	27
7.1 Introduction-----	27
7.2 The Single-Source Loop Inductor-----	28
7.3 A Double-Source Loop Inductor-----	29
7.4 A Quadruple-Source Loop Inductor-----	30
7.5 A Loop Inductor with a Continuously-Distributed Source-----	31
 <u>APPENDIX B</u>	
8. METHODS USED TO SIMULATE THE MULTIPLE SOURCES-----	33
8.1 Introduction-----	33
8.2 The Shielded Half-Loop with a Gap at One End-----	33
8.3 The Shielded Half-Loop with a Gap at the Center-----	35
8.4 The Shielded Quarter-Loop with a Gap at the Center-----	35
8.5 Calculation of the Loop Characteristics-----	37
9. REFERENCES-----	39

## LIST OF FIGURES

	<u>Page</u>
Fig. 1 Diagram of the Magnetic-Field Generator-----	6
Fig. 2 View of the Four-Gap Loop Inductor-----	7
Fig. 3 View of the Inductor and Matching Networks-----	8
Fig. 4 Circuit Diagram of the Matching Network-----	9
Fig. 5 View of the Matching Network-----	10
Fig. 6 View of the Toroidal Balun Transformer-----	13
Fig. 7 A Basic Balun Circuit-----	14
Fig. 8 Winding the Toroidal Balun Transformer-----	14
Fig. 9 Diagram of the Near-Field Synthesizer-----	16
Fig. 10 View of the Near-Field Synthesizer-----	17
Fig. 11 Circuit Diagram of the Matching Network-----	18
Fig. 12 Diagram of the Complete Synthesizer-----	22
Fig. 13 Diagram of the Phase-Shift Network-----	23

### APPENDIX A

Fig. 14 Single-Source E-Field Distribution-----	29
Fig. 15 Double-Source E-Field Distribution-----	30
Fig. 16 Quadruple-Source E-Field Distribution-----	30
Fig. 17 Continuous-Source E-Field Distribution-----	32

### APPENDIX B

Fig. 18 Half-Loop with a Gap at One End-----	34
Fig. 19 Half-Loop with a Gap at the Center-----	36
Fig. 20 Quarter-Loop with a Gap at the Center-----	36

DEVELOPMENT AND CONSTRUCTION OF AN ELECTROMAGNETIC  
NEAR-FIELD SYNTHESIZER

Frank M. Greene

ABSTRACT

This publication describes work done by the National Bureau of Standards for the USAF School of Aerospace Medicine at Brooks AF Base involving the development, design, construction and testing of a prototype EM near-field synthesizer. The purpose of the contract was to provide a means of independently generating high-level electric and magnetic near fields in the frequency range 10 to 30 MHz. These fields are to be used in various ratios by the USAFSAM in their EM radiation exposure program for determining the biological effects of hazard-level non-ionizing EM fields on human beings.

The synthesizer consists of a balanced, parallel-plate strip line to generate the "desired" electric field, and a single-turn quadruple-feed inductor placed parallel to and midway between the plates to generate the "desired" magnetic field. Methods used to reduce the "unwanted" E- and H-field components associated with the above, as well as the methods used to reduce the coupling between the two field systems are discussed. The result is a synthesizer in which the electric- and magnetic-field components can be adjusted essentially independently over wide ranges of magnitude, relative time-phase, and spatial orientation to simulate various near-field configurations.

Previous research has been largely limited to the use of plane-wave fields for evaluating RF biological hazards. This new device will allow researchers to investigate any near-field effects that may occur at high field levels.

Keywords: Electromagnetic-field hazards; electromagnetic-field synthesizer; electromagnetic radiation-exposure testing (non-ionizing); near fields; RF biological hazards.

## 1. INTRODUCTION

This publication describes work done by the National Bureau of Standards for the USAF School of Aerospace Medicine at Brooks Air Force Base involving the development, design, construction, and testing of a prototype EM near-field synthesizer. The purpose of the contract was to provide a means of independently generating high-level electric and magnetic near-fields in the frequency range 10 to 30 MHz. These fields are to be used in various ratios by the USAFSAM in their EM radiation exposure program for determining the biological effects of hazard-level non-ionizing EM fields on human beings.

The synthesizer consists of: (a) a balanced, parallel-plate strip line to generate the "desired" electric field; and (b) a single-turn quadruple-feed inductor placed parallel to and midway between the plates to generate the "desired" magnetic field. It is generally known from Maxwell's equations that in addition to the "desired" E and H fields in (a) and (b) respectively, the electric field in (a) is accompanied by an "unwanted" magnetic field, and the magnetic field in (b) is accompanied by an "unwanted" electric field.

It turns out that the "unwanted" magnetic field produced by the parallel-plate strip line is negligibly small for the plate size, frequency, and the magnitude of E being used. It will be shown how the magnitude of the "unwanted" E-field produced by the single-turn inductor was reduced by an order of magnitude in the central portion of the inductor by the expediency of using a multiple-feed rather than the conventional single feed. This means that under the conditions of use the single-turn inductor can generate a fairly "pure," high-level H-field, and the parallel-plate line a fairly "pure," high-level E-field over the above frequency range.

The electric and magnetic coupling between the two field systems was minimized by operating each system in a balanced mode and with the required mutual symmetry. There is no observable cross-coupling even when the loop is rotated out of its initial plane of symmetry by any desired angle. As a result, the electric- and magnetic-field components can be adjusted essentially independently over wide ranges of magnitude, relative electrical time-phase, and relative spatial orientation in order to simulate various near-field configurations. The maximum RF driving power required is one kilowatt for each field system.

Previous research in RF biological hazards has been largely limited to the use of plane-wave fields for making clinical studies. This new device will allow researchers to investigate any near-field effects that may occur at high-field levels. The practical mks International System of Units (SI) is used throughout this paper.

## 2. THE RF MAGNETIC-FIELD GENERATOR

**2.1 The Physical Characteristics of the Loop Inductor.** The RF magnetic-field generator consists basically of a single-turn inductor having an average diameter of 21 5/8" (54.9 cm) formed from copper tubing having an outside diameter of 1 5/8" (41.3 mm) and a wall thickness of 1/16" (1.59 mm). The inductor has a low-frequency inductance of 0.921 microhenry as determined from Equation (2) in Appendix A. The diameter selected was the result of a compromise to make the inductor as small as possible (to maintain a reasonably high self-resonant frequency) while still providing sufficient space to accomodate the primate during exposure without undue crowding. Large-sized copper tubing was used to minimize the RF conductor losses and consequently the RF driving power requirements of the source, as well as for reasons of mechanical strength.

The choice of a single-turn rather than a multiple-turn inductor was made because of the following desirable characteristics:

- (a) a lower distributed capacitance;
- (b) a higher resultant self-resonant frequency;
- (c) a lower "unwanted" electric-field strength due to a lower reactive voltage drop; and
- (d) less shielding of the "desired" electric field of the associated parallel plates previously mentioned. This shielding would in effect produce a distortion of the spatial distribution of the "desired" electric field which would increase with the number of turns of the inductor.

All joints in the loop are high-temperature silver-brazed to provide maximum electrical conductivity, mechanical strength, and water tightness (for cooling to be discussed later).

2.2 The Electrical Characteristics of the Loop Inductor. The inductor is driven, in effect, by four synchronous RF generators located symmetrically 90 degrees apart around the loop periphery [1,2]. While these generators are in-phase with respect to each other, diametrically-opposite generators create electric fields which are spatially 180 degrees out of phase and therefore cancel at the center of the inductor. This provides for an order-of-magnitude (10:1) reduction in the "unwanted" electric field that would otherwise exist in the central portion of the loop if driven by only one generator as shown in Appendix A. The magnetic field remains unaffected since only those components of the electric field that do not contribute to  $\text{Curl } \vec{E}$  are being cancelled as will be discussed later.

Instead of a single gap as found in the usual "shielded" loop [3,4], this loop has four gaps (90 degrees apart) as

shown in Figure 1. The four driving voltages are fed-in coaxially and appear across the respective gaps, in-phase with respect to each other. The inner conductor of the co-axial drive is 3/4" (19.1 mm) diameter copper tubing with a 1/32" (0.794 mm) wall thickness. With the electrical balance or symmetry that must be maintained around the periphery of the four-gap loop, four voltage nulls or zero-potential points result, one midway between each of the four gaps. These null points lie on two orthogonal image planes intersecting at the center of the loop. This permits the loop to be both mounted mechanically and driven electrically from two diametrically opposite null points as indicated in Figure 1. Since each of the matching networks shown has a balanced (push-pull) output, each, in effect, provides two of the four driving voltages, discussed above, in the proper phase relationship. An exploded view of the four-gap loop inductor and the coaxial inner conductors is shown in Figure 2. A view of the assembled loop inductor and its associated matching networks is shown in Figure 3.

The "unwanted" electric-field in the plane of the loop is proportional to both the operating frequency and the distance from the center,  $r$ , as shown by Equation (7) in Appendix A. For a magnetic field strength of 50 amperes per meter, as specified by the sponsor, the electric field at a distance,  $r$ , equal to one-quarter of the loop radius, varies from approximately 130 volts per meter at 10 MHz to 400 volts per meter at 30 MHz. This has been found to be approximately an order of magnitude lower than would be the case if only a single driving generator were used as shown in Figures 14 and 16 in Appendix A. The magnetic-field generator is designed to produce a field strength of up to 100 amperes per meter with a transmitter RF power output of up to one kilowatt which is the maximum RF power capability of the units supplied by NBS.

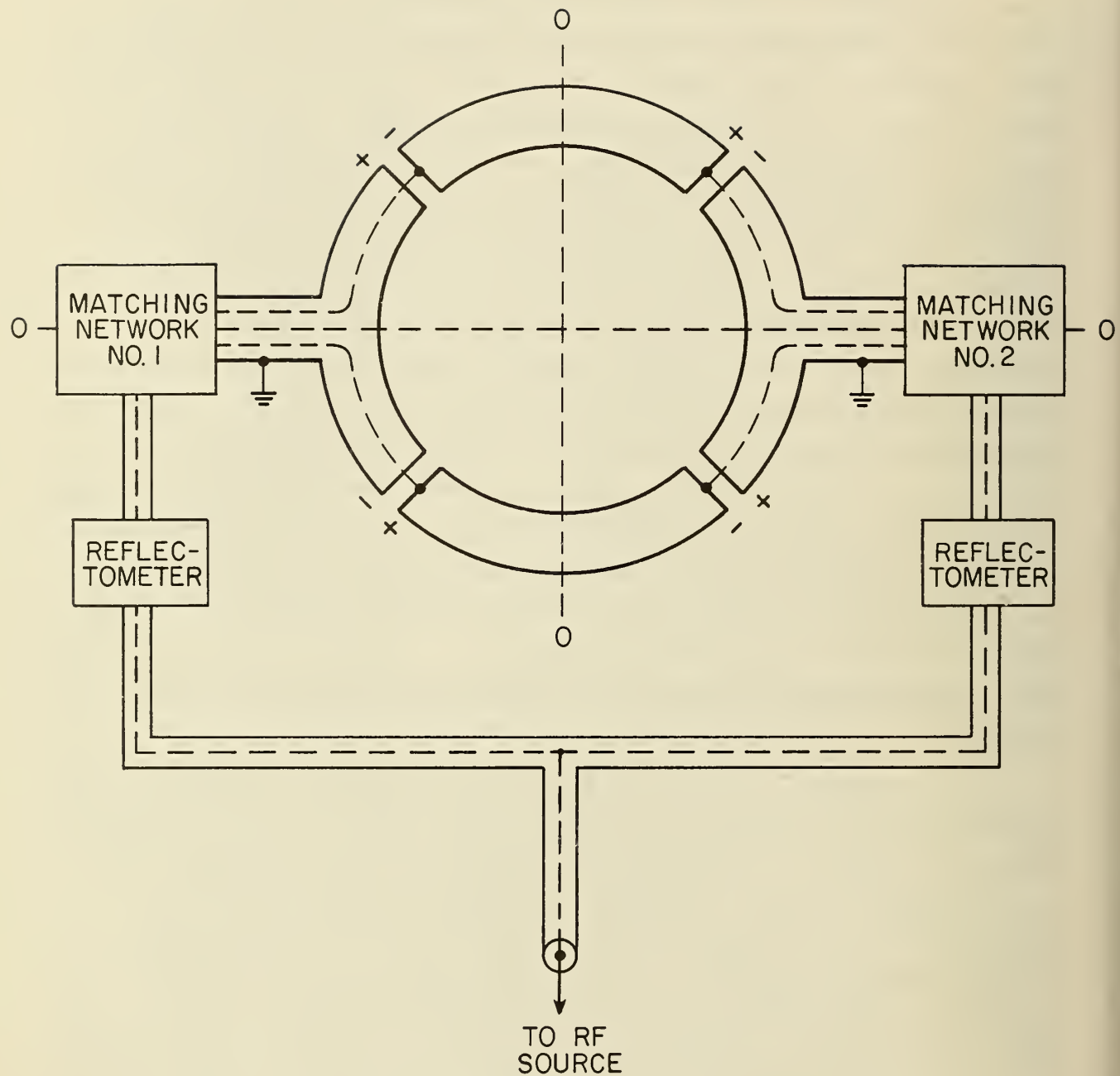


Figure 1. A Block Diagram of the RF Magnetic-Field Generator Showing the Four-Gap Shielded-Loop Inductor and the Associated Tunable Matching Networks for Use from 10 to 30 MHz. The Two Orthogonal Image Planes are Shown Intersecting at the Center of the Loop.

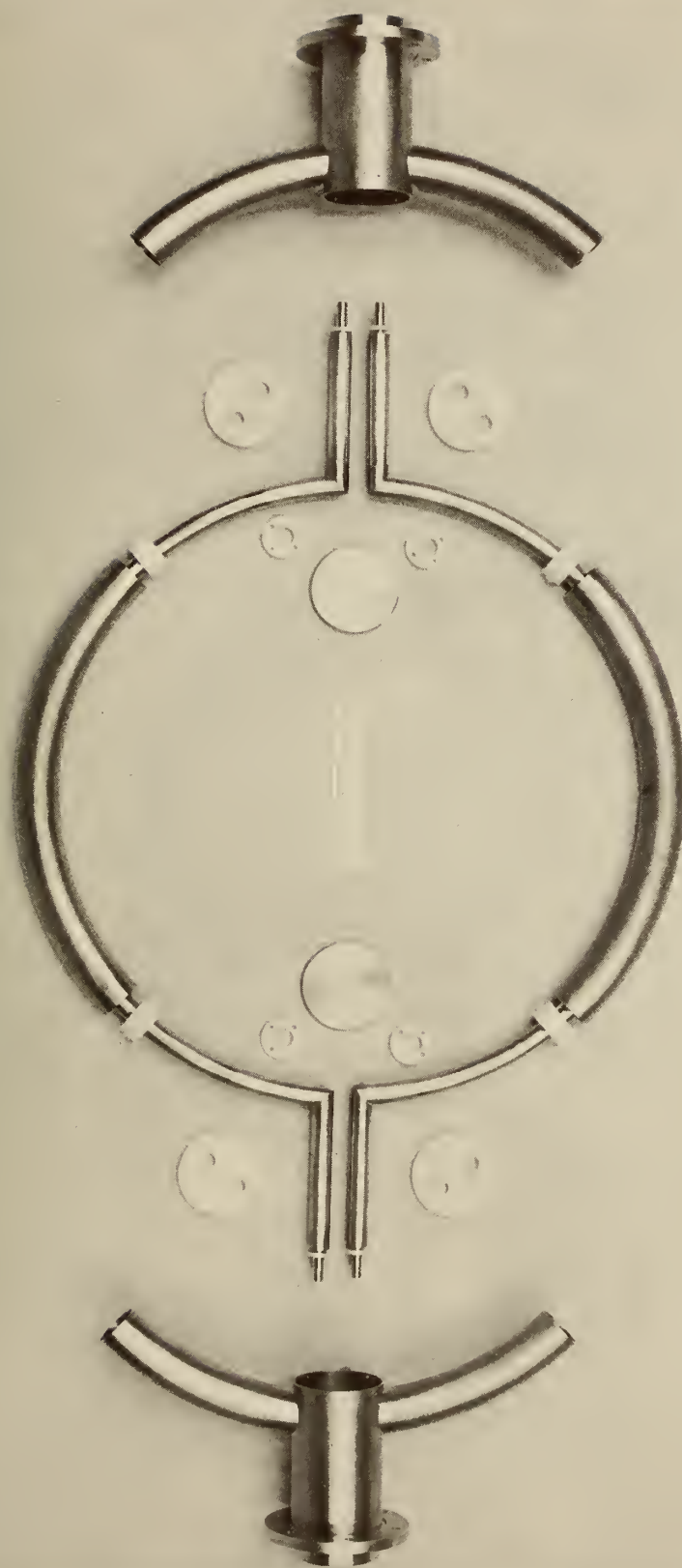


Figure 2. An Exploded View Showing the General Construction of the Four-Gap Shielded Loop Inductor. The Four Water Nozzles Can Be Seen at the Extreme Ends of the Center Conductors for Use in Water-Cooling the Loop.



Figure 3. An Assembled View of the RF Magnetic-Field Generator Showing the Shielded-Loop Inductor and the Two Integral Matching Networks with Covers Removed.

2.3 The Loop-Inductor Matching Networks. The two balanced, tunable networks provide for impedance matching between the loop inductor and driving generator over the frequency range 10 to 30 MHz. The circuit diagram of one of the two identical matching networks is shown in Figure 4, and comprises vacuum variable capacitors C-1 and C-2, and inductor L-1. A separate

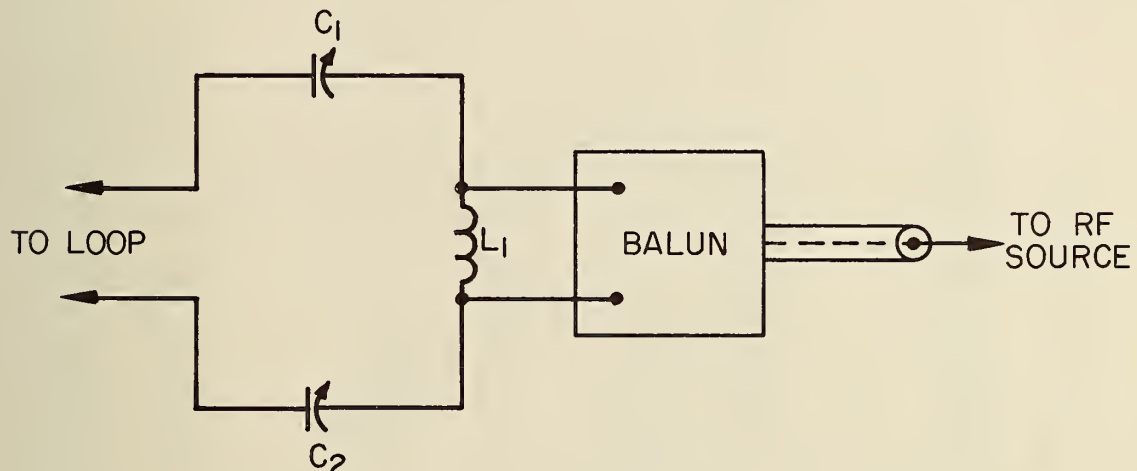


Figure 4. The Circuit Diagram of One of the Two Identical Matching Networks Used with the Shielded Loop Inductor.

balun transformer is also provided, as shown, between the 300-ohm balanced input to each network and its 75-ohm coaxial transmission line. The coaxial input circuits of the two matching networks are driven in parallel from a common source as shown in Figure 1. A close-up view of one of the matching networks is shown in Figure 5.

The loop inductor, and inductor L-1 in Figure 4, are tuned to resonance at the desired operating frequency by the capacitors, C-1 and C-2, each of which has a range of adjustment from 10 to 1000 pF. The balanced input impedance is determined by the value selected for inductor, L-1, in a manner exactly analogous to that employed when using a tapped, tuned tank circuit. When properly resonated the input impe-

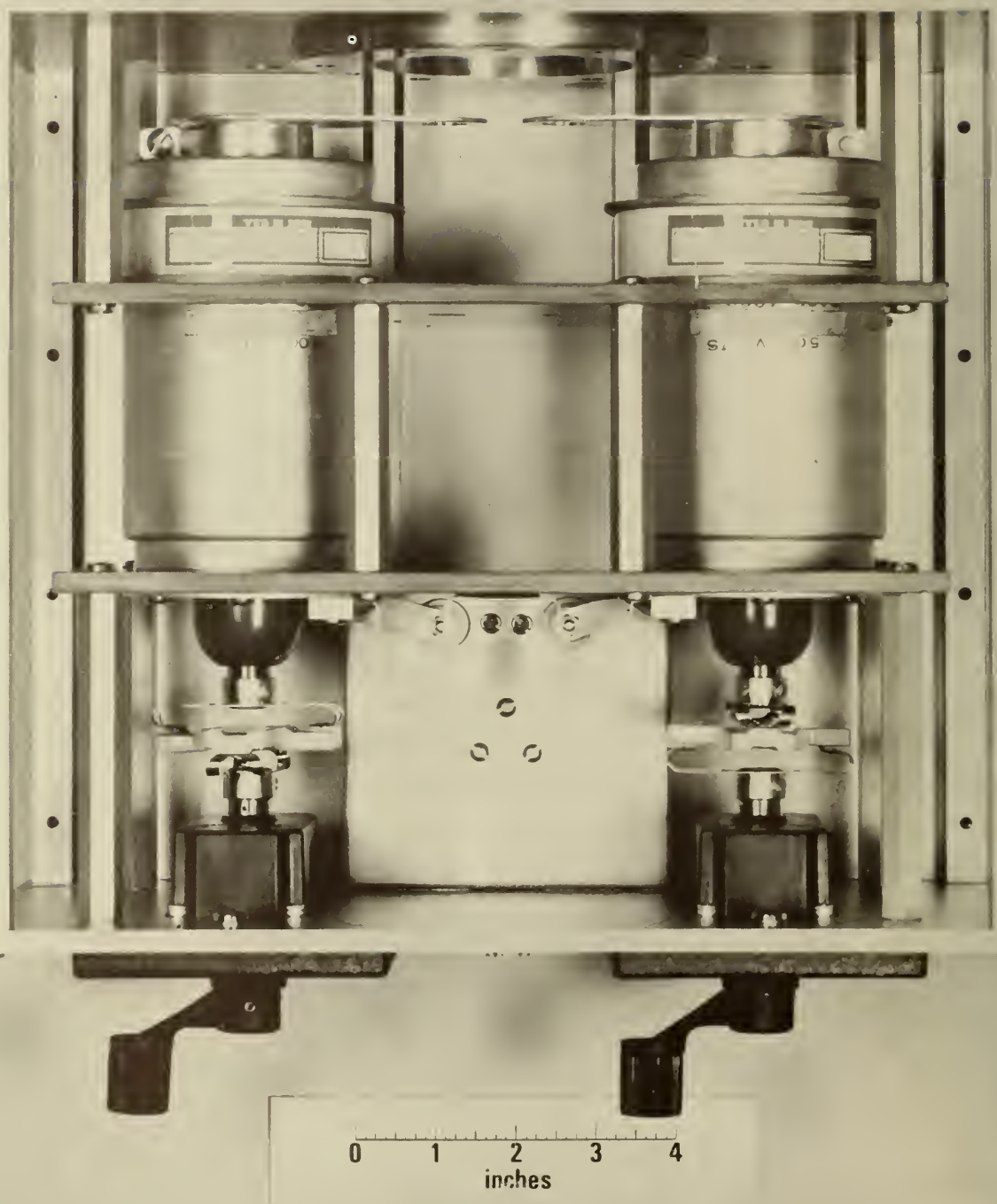


Figure 5. A View of One of the Tunable Loop-Inductor Matching Networks Showing the Two Vacuum Capacitors and the Shielded Balun Transformer.

dance,  $Z_{in}$ , is purely resistive and is given to a good approximation [5] by the following expression (provided  $Q \geq 10$ ):

$$Z_{in} \approx \frac{X_L^2}{R}, \text{ ohms,} \quad (1)$$

where  $X_L$  is the reactance of the inductor, L-1, at the resonant frequency, and R represents half the total equivalent series loss resistance of the loop circuit, including conductor, dielectric, and radiation losses. The latter is assumed negligible as will be discussed later. This means that essentially all of the input RF driving power to the loop will be converted into heat and dissipated in the loop and associated circuitry.

**2.4 The Vacuum Variable Tuning Capacitors.** The vacuum variable capacitors used in the loop-inductor matching networks have the following advantages over conventional air variable capacitors for this type of use:

- (a) a larger absolute capacitance as well as a larger range of capacitance adjustment (ratio of maximum to minimum capacitance) for a given physical size;
- (b) a higher RF voltage breakdown rating;
- (c) lower RF losses and heating and therefore a higher RF current rating. The RF current rating for a given frequency can be limited by either the RF heating, or by RF voltage breakdown resulting from the reactive voltage drop;
- (d) a lower internal inductance, and therefore a higher self-resonant frequency.

**2.5 The Balun Transformer [6].** The toroidal balun transformer used in each of the networks converts the 300-ohm balanced-network input impedance to a 75-ohm unbalanced coaxial drive.

The balun has an RF power rating of 1 kilowatt continuous at 99 percent efficiency (.05 dB insertion loss). A view of the balun is shown in Figure 6. The winding arrangement is shown in Figures 7 and 8. Copper ribbon 0.013" (0.330 mm) thick by 0.100" (2.54 mm) wide is used which is the equivalent of No. 14 AWG (0.064" = 1.63 mm dia) copper wire in electrical conductivity in this frequency range and is much easier to wind physically. The balun is wound on a ferrite toroidal core approximately 2-1/2" (63.5 mm) O.D. x 1-1/2" (38.1 mm) I.D. x 1.0" (25.4 mm) thick which has an initial relative permeability of approximately 40 for frequencies up to at least 30 MHz. The purpose of the core is to increase the common-mode rejection at the lower frequencies. The transformer has a measured common-mode rejection of approximately 30 dB over the frequency range 10 to 30 MHz.

The winding directions are important and are as shown in Figure 8. The common-mode currents,  $I_c$ , in the two transmission lines magnetize the core in the directions shown by the arrows. Since the magnetic flux produced by these currents in the two lines is in the same direction in the core, this results in a maximum common-mode inductance. The balanced-mode currents in the two sides of each transmission line are equal in magnitude and opposite in phase. They therefore produce very little, if any, magnetization of the core and hence no balanced-mode inductance. The core therefore has little, if any, effect on the two transmission lines operating in the balanced mode and serves only to attenuate the common-mode currents. As a result, there is little, if any, RF core loss in normal operation. The losses are essentially all in the copper windings, which helps to explain the high operating efficiency.

2.6 The Water Cooling of the Inductor. The loop inductor is designed to be water-cooled, since the measured RF driving

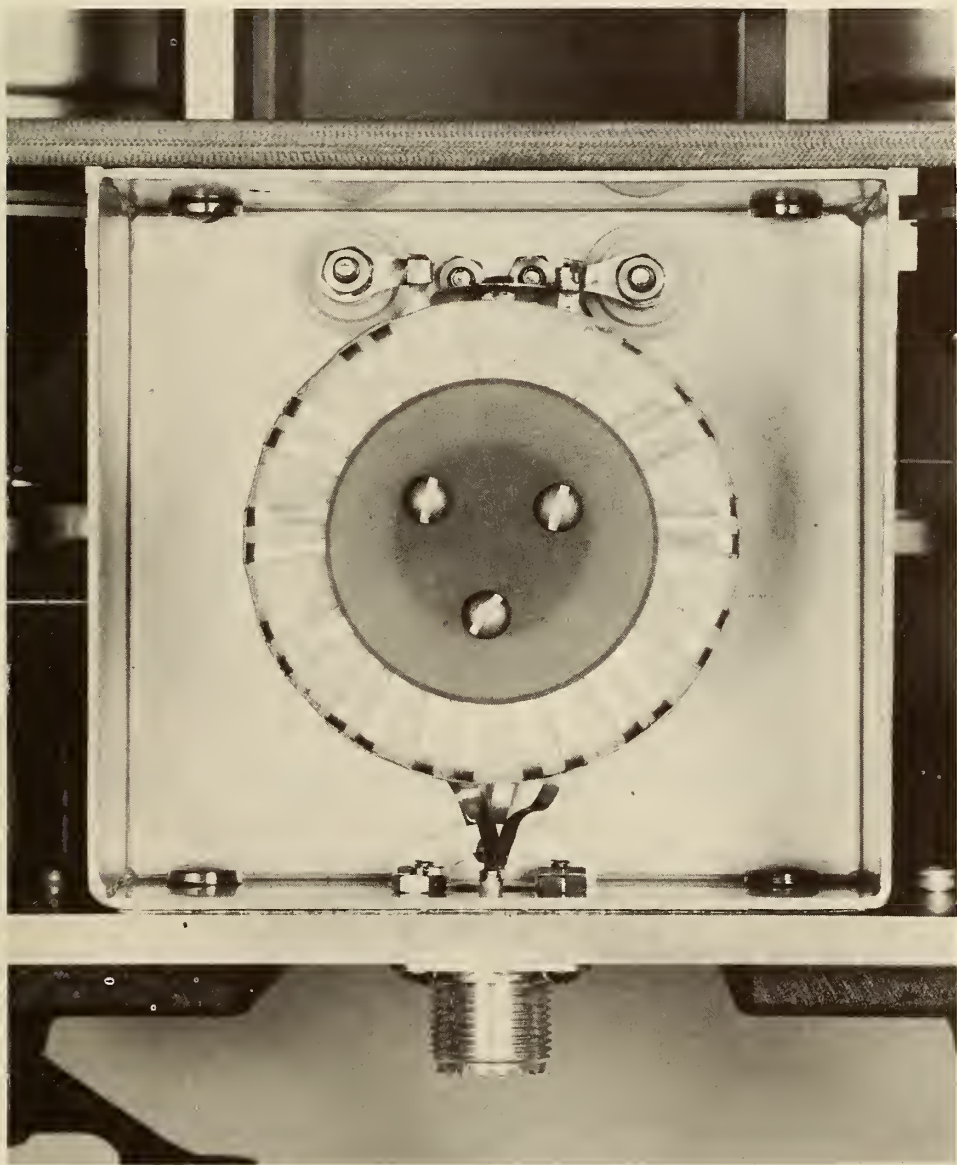


Figure 6. A Bottom View of One of the 75 to 300 Ohm Toroidal Balun Transformers Used in the Loop-Inductor Matching Networks.

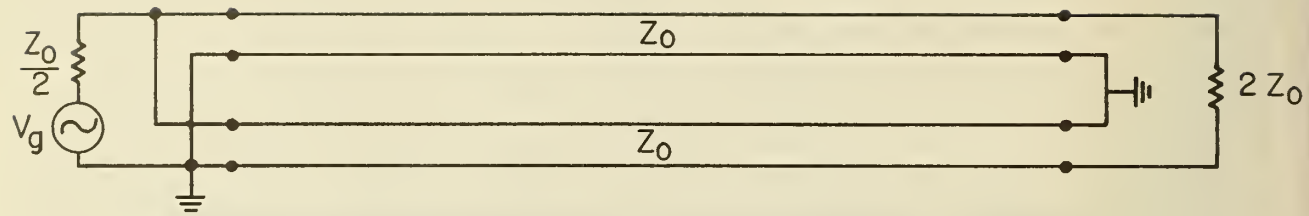


Figure 7. A Basic Balun Circuit Comprising Two Balanced Transmission Lines of Characteristic Impedance,  $Z_0$ . The Lines are Connected in Parallel at One End and in Series at the Other, Giving an Impedance Transformation Ratio of 4:1.

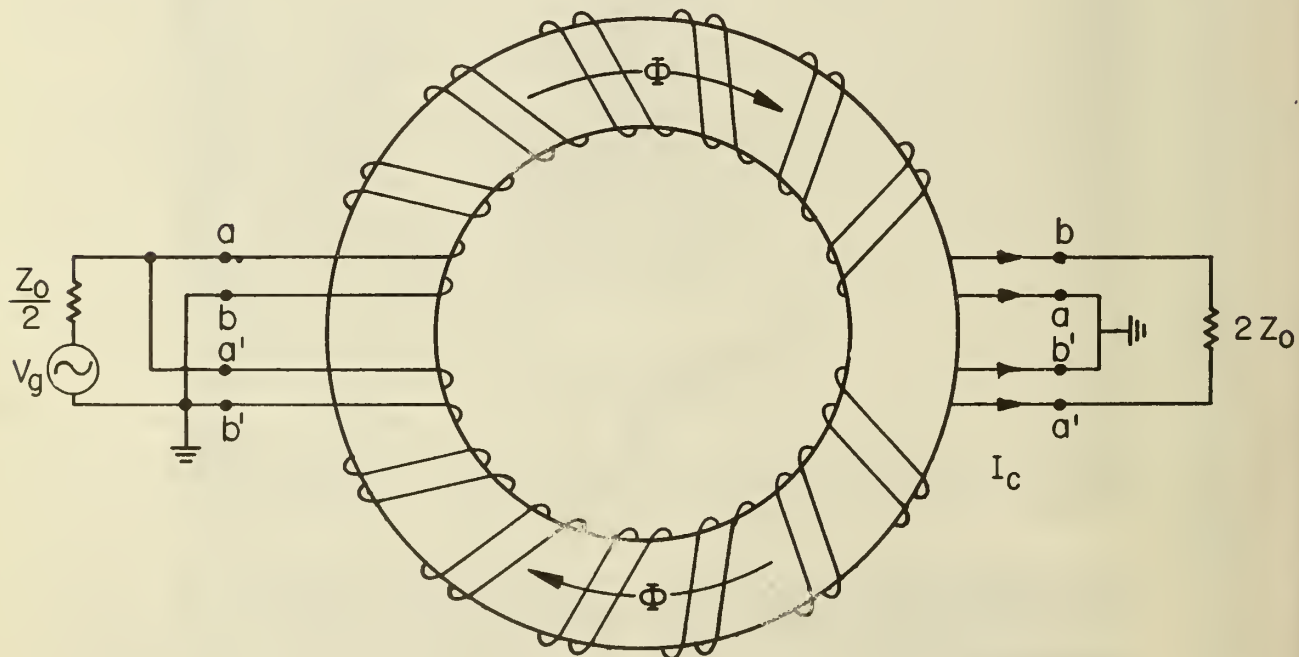


Figure 8. The General Method of Winding Used in the Toroidal Balun Transformer. The Basic Arrangement is the Same as that of Figure 7, Except that the Transmission Lines Have Been Wound on a Toroidal Core to Increase the Common-Mode Rejection at the Lower Frequencies.

power required to overcome circuit losses and produce a magnetic field of 50 amperes per meter is in the range from approximately 175 watts to over 500 watts over the operating frequency range 10 to 30 MHz. A 1/2" (12.7 mm) O.D. plastic water hose connects to the nozzles which can be seen in Figures 2 and 3 at the extreme ends of the center conductors. Only a minimal amount of water flow is required to keep the loop at room temperature (approximately 1 quart (0.95 liter) per minute which can be obtained with ordinary tap pressure is sufficient). Water cooling is necessary for two reasons: (a) it eliminates any possible effect of an increase in the ambient air temperature on the primates during exposure; and (b) it stabilizes the loop tuning which otherwise drifts appreciably as the loop heats up. The water flows through the interior of the loop center-conductor and so is essentially not in contact with the electrical part of the circuit. This is true except at points of entry and exit where the length of the water column is sufficient to minimize any shunting effect.

### 3. THE RF ELECTRIC-FIELD GENERATOR

3.1 The Physical Characteristics of the Parallel-Plate Strip Line. The RF electric-field generator consists of a balanced parallel-plate strip line fabricated from 1/16" (1.59 mm) thick aluminum sheets approximately 30" (75 cm) wide and spaced the same distance apart. The line is also approximately 30" (75 cm) in length along the straight portion, and tapers both in width and spacing over a distance of approximately 20" (50 cm) on the driven end as shown in Figure 9. This permits connecting the balanced RF feed line with a minimum of electrical discontinuity. Connection is made to the balanced strip line by means of two large feed-through bushings using

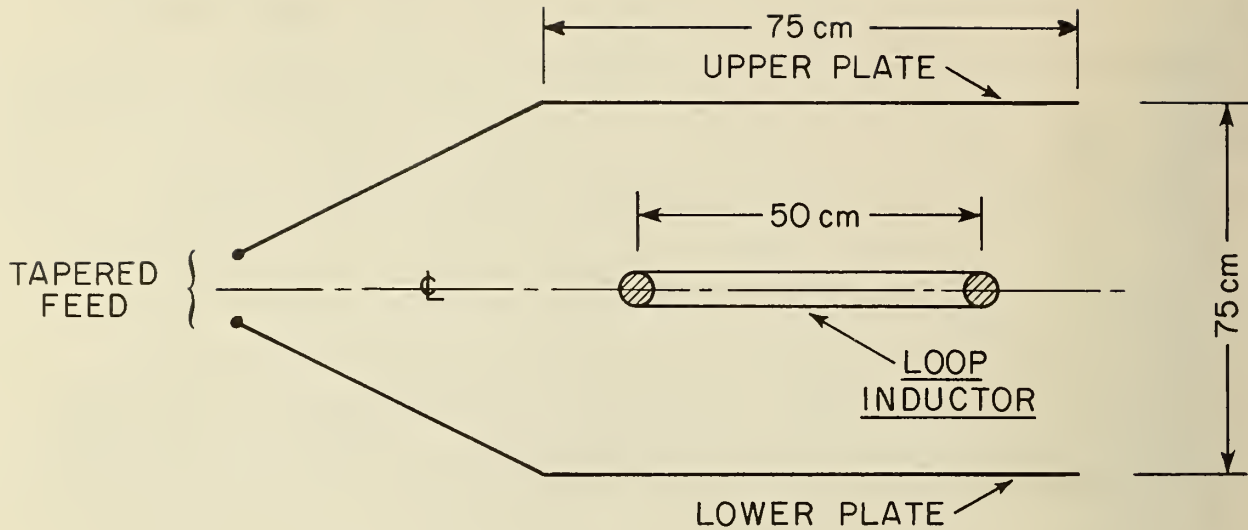


Figure 9. The General Arrangement of the EM Near-Field Synthesizer. The Loop Inductor is Located Midway between the Balanced Parallel Plates Normally in the Neutral Plane, but can be Tilted at Any Angle up to 60 Degrees.

steatite insulating cones. These pass through a metal plate on one side of the shielded room in which the synthesizer is located and into the tunable matching unit which is fastened to the outside. A view of the strip-line is shown in Figure 10.

3.2 The Parallel-Plate Matching Network. A balanced, tunable network is provided for impedance matching between the parallel plates and the driving generator. The network is housed in a large aluminum box 20" (50.8 cm) x 20" (50.8 cm) x 18" (45.7 cm) fastened to the outside center of the shielded room in which the synthesizer is operated. Electrical connection is made to the parallel plates by means of the two large feed-through bushings previously mentioned. The size of the housing is dictated by the size of the tuning coils employed in order to obtain maximum Q and RF power-handling capability. A small muffin fan is used to exhaust air from a vent in the top side of the enclosure to facilitate cooling the inductors of the

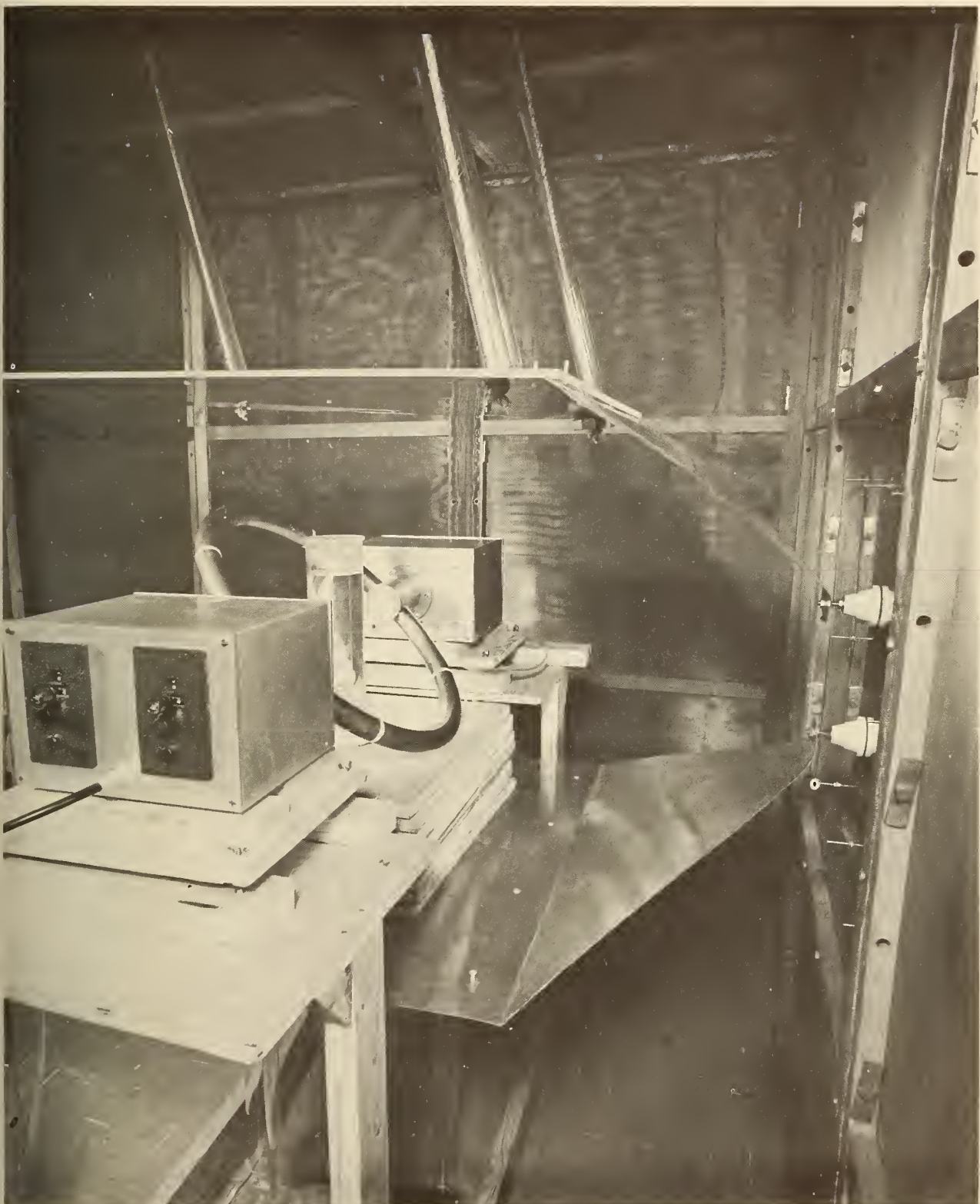


Figure 10. A View of the Electromagnetic Near-Field Synthesizer as Installed in the Shielded Room. The Parallel-Plate Strip Line and the Four-Gap Loop with its Matching Networks can be seen.

matching network. A matching air inlet is provided in the bottom of the enclosure to ensure proper air circulation.

The circuit diagram of the matching network is shown in Figure 11. The parallel plates are tuned to resonance at the

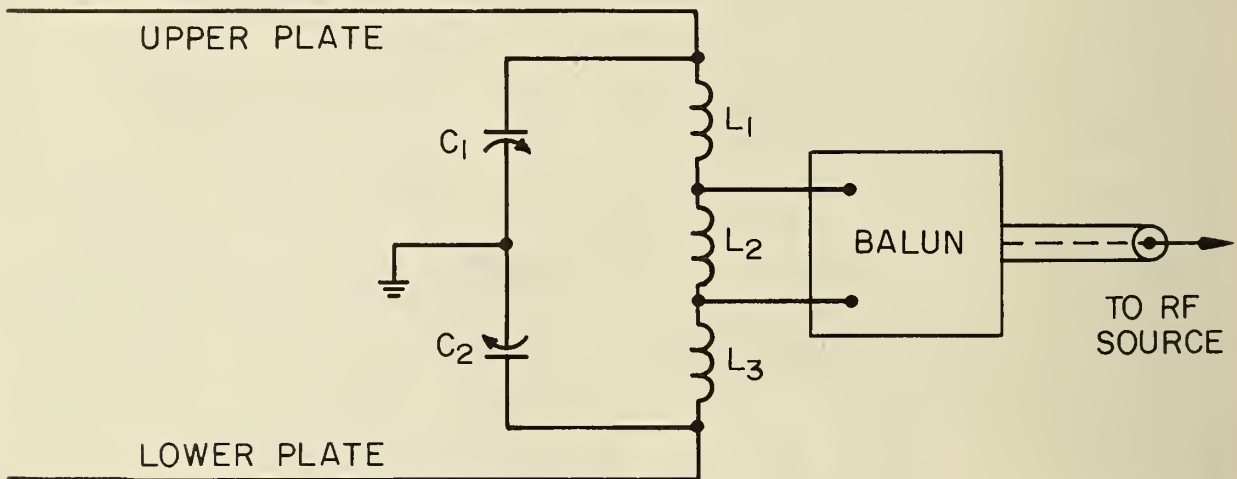


Figure 11. The Circuit Diagram of the Parallel-Plate Matching Network.

desired operating frequency by the balanced inductance comprised of  $L_1$ ,  $L_2$ , and  $L_3$ . The two vacuum variable capacitors,  $C_1$  and  $C_2$ , facilitate the tuning. Each has a range of adjustment from 6.5 to 50 pF. The input impedance is determined by the value selected for inductance  $L_2$  in exactly the same manner as previously described for the magnetic-field generator, and can be determined from Equation (1), Section 2.3.

A toroidal balun transformer is used as shown in the circuit diagram to convert the 300-ohm balanced-network input impedance to a 75-ohm unbalanced coaxial drive. The transformer is identical to those used with the loop matching networks.

3.3 The Electrical Characteristics of the Parallel-Plate Strip Line. The "unwanted" magnetic field produced by the parallel plates was found to be negligibly small for the plate size, frequency, and the magnitude of the electric field,  $E$ , being generated. No special design was undertaken to minimize this "unwanted" magnetic field as was done in the case of the loop inductor. Although, it would have been possible to have reduced the magnetic field in the central portion of the parallel plates by a factor of at least three, if necessary, by driving the plates simultaneously [7] at both ends instead of at one end.

An RF driving power of between approximately 150 and 300 watts is required over the frequency range of 10 to 30 MHz to produce an electric field strength of 5000 volts per meter between the plates as required by the sponsor. This is the power required to supply the conductor and dielectric losses of the parallel plates and associated circuitry, the radiation losses again being negligible because of the mode of operation, as in the case of the loop inductor. Because of the surface area involved in the parallel plates, their losses are minimal. Little temperature rise was observed, and no cooling was found necessary. Most of the loss was found to be in inductors L-1, L-2, and L-3 (Figure 11).

The electric-field generator is designed to produce a field-strength of up to 10,000 volts per meter with a transmitter RF power output of up to one kilowatt which is the maximum RF power capability of the units supplied by NBS.

#### 4. THE COMPLETE SYNTHESIZER UNIT

4.1 A General Description. In the completed EM near-field synthesizer the single-turn loop inductor of the magnetic-field generator is mounted midway between and parallel to the two

balanced plates of the electric-field generator as shown in Figure 9. The normal position of the loop inductor is thus in the neutral plane between the plates, although the loop can be operated at any angle to the horizontal of up to 60 degrees. This provides the means for adjusting the relative spatial orientation between the electric and magnetic field vectors as specified by the sponsor. The electric and magnetic coupling between the two field systems has been minimized because of the balanced symmetry employed in the excitation of both the loop inductor and the parallel plates, as well as their relative physical orientation. This was confirmed during the acceptance tests at Brooks Air Force Base in which no observable cross coupling could be detected even with power inputs of up to one kilowatt to either or both the field generators for any angular position of the loop inductor up to 60 degrees from the horizontal.

4.2 The Effect of the Shielded Room. The near-field synthesizer is installed and operated inside of a doubly-shielded copper room approximately 7 ft (2.13 m) wide x 10 ft (3.05 m) long x 8 ft (2.44 m) high. The RF power required to drive either the electric- or magnetic-field generator has been found to be the result mainly of losses within the generators and matching networks themselves (i.e. metallic and dielectric losses in the inductors, capacitors, parallel plates, etc.). Radiation losses are, for the most part, nonexistent because of operation of the generators inside a copper-shielded room having a shielding efficiency of at least 60 dB. Coupling between each field generator and the interior walls of the screened room has been found to be very loose and is essentially reactive. Very little resistance is coupled back into the field generators from the room walls, since: (a) the copper walls of the room are low-loss; (b) the physical

dimensions of the generators are small compared to the room dimensions; and (c) the frequency of operation is well below the lowest possible self-resonant frequency of the shielded room operating as a low-loss rectangular cavity resonator. For this room the lowest possible self-resonant frequency [8] is approximately 80 MHz.

4.3 The RF Excitation of the Field Generators. The two field generators are driven or excited as shown in the block diagram of Figure 12. Separate, synchronized, transmitters are used, each of which is composed of a 100-watt driver transmitter followed by a one-kilowatt RF power amplifier as shown. Synchronization is achieved by operating both 100-watt driver transmitters from the same crystal oscillator. Separate frequencies can be easily used for each transmitter if for any reason it is desired. Reflectometers are provided, as shown, to facilitate tuning the two systems. It is found advantageous to first tune the loop-inductor and the parallel plates so as to have the correct input impedance, using one of the new RF vector-impedance meters supplied by NBS.

4.4 The Phase-Shift-Networks. Two pi-type phase-shift networks [9] were designed and constructed at NBS to provide for an adjustable time-phase difference between the electric and magnetic fields generated, in addition to the adjustable spatial orientation provided. These units are identical in size and appearance to the two impedance matching networks provided with the loop-inductor as shown in Figure 5. They provide for phase shifts from 30 to 150 degrees each over the frequency range 10 to 30 MHz. They can be used singly or in tandem to provide a total phase shift of up to 300 degrees if desired. The circuit diagram of the phase-shift networks is shown in Figure 13.

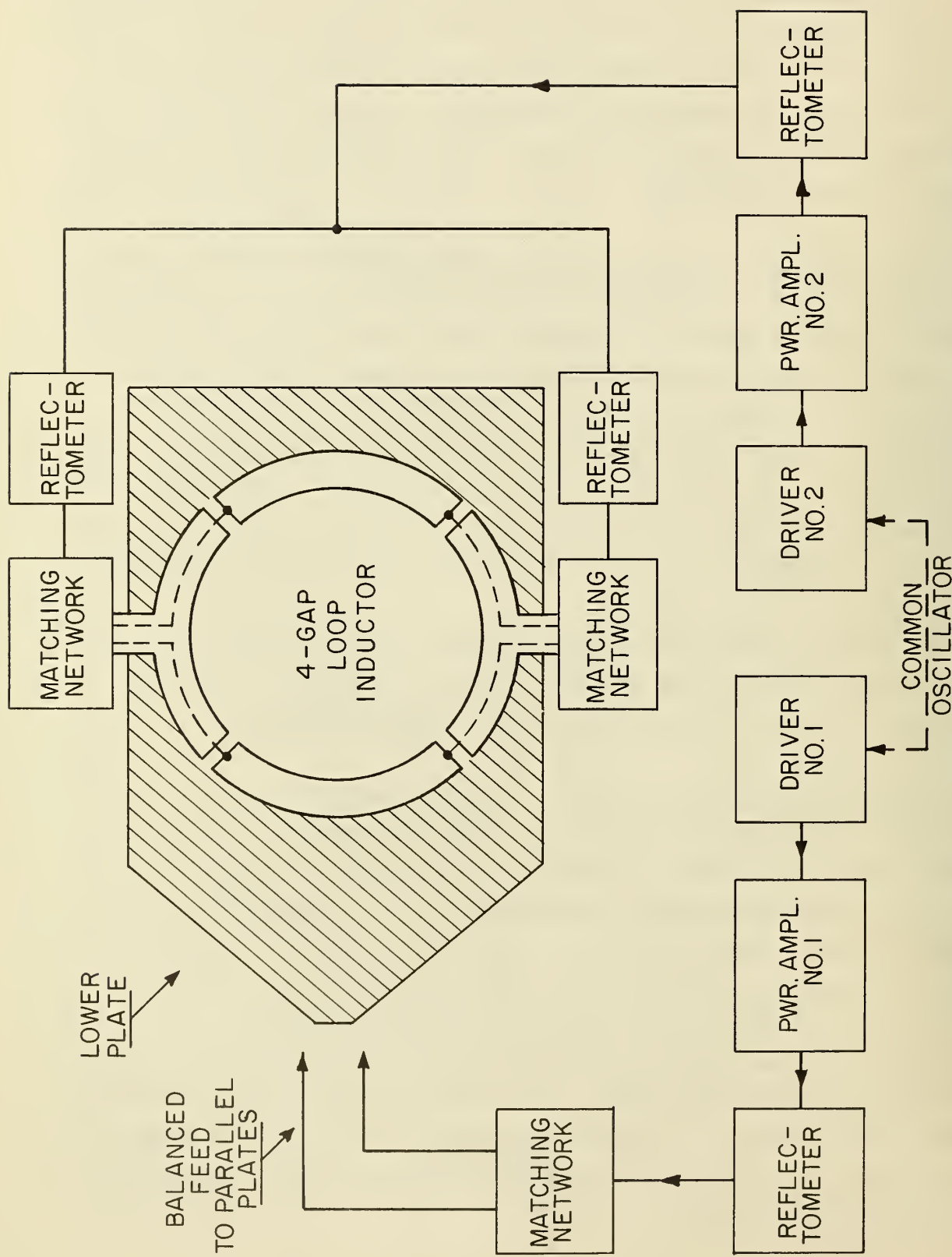
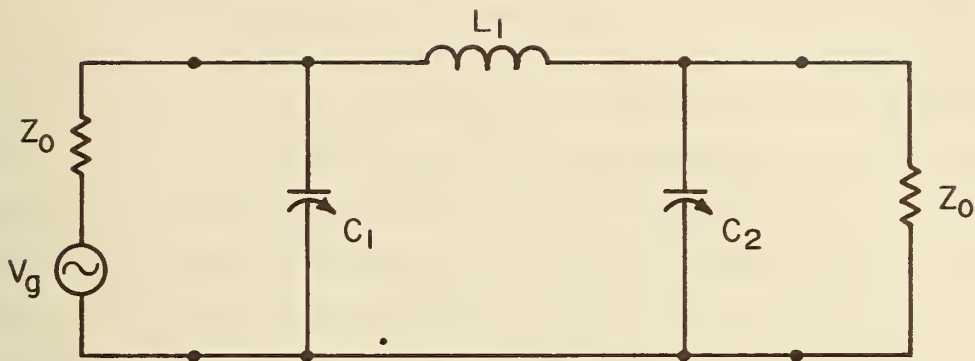


Figure 12. A Block Diagram of the Complete EM Near-Field Synthesizer Showing all of the Principal Components Including the RF Power Sources.



**Figure 13.** The Circuit Diagram of the Pi-Type Phase-Shift Networks Used with the EM Near-Field Synthesizer. These are Similar to a Pi-Type Impedance-Matching Network Except they are Inserted in an Already-Matched System to Produce an Insertion Phase Shift Without Disturbing the Match.

**4.5 The RF Exposure Capability.** The electric-field generator can produce a fairly pure (high-impedance) E field of up to 10,000 volts per meter over the frequency range 10 to 30 MHz. The magnetic-field generator can produce a fairly pure (low-impedance) H field of up to 100 amperes per meter over the same frequency range. The two fields can be adjusted essentially independently in amplitude. As a result, the ratio of the magnitude of the electric field to that of the magnetic field can be adjusted to any value between roughly 40 and 4000. The electrical time-phase difference between E and H can be adjusted for angles up to 300 degrees, and relative spatial orientation for angles up to 60 degrees in order to simulate various near-field configurations. An RF driving power of up to one kilowatt is required for each field system depending upon frequency and the field level used.

## 5. SUMMARY AND CONCLUSIONS

This publication describes the development, design, construction and testing of a prototype EM near-field synthesizer conducted by the National Bureau of Standards for the USAF School of Aerospace Medicine at Brooks Air Force Base. The purpose of the contract was to provide a means of independently generating high-level electric and magnetic near-fields in the frequency range 10 to 30 MHz. These fields are to be used in various ratios by the USAFSAM in their EM radiation exposure program for determining the biological effects of hazard-level, non-ionizing EM fields on human beings.

The synthesizer consists of: (a) a balanced parallel-plate strip line to generate the "desired" electric field; and (b) a single-turn quadruple-feed inductor placed parallel to and midway between the plates to generate the "desired" magnetic field. It is generally known from Maxwell's equations that in addition to the "desired" E and H fields in (a) and (b) respectively, the electric field in (a) is accompanied by an "unwanted" magnetic field, and the magnetic field in (b) is accompanied by an "unwanted" electric field.

In order to obtain essentially independent control over the amplitudes of the "wanted" electric and magnetic fields as produced above, it was necessary to reduce the "unwanted" field components insofar as possible. It was shown how the "unwanted" electric field associated with a single-turn loop inductor was reduced in magnitude in the central portion of the loop by as much as a factor of ten by increasing the number of in-phase RF sources feeding the loop from one up to four. It was also shown that the four-source loop was probably the optimum from a practical standpoint, and the design of such a loop was described in detail. It was found that the "unwanted" magnetic field produced by the parallel-plate strip

line was negligibly small for the plate size, frequency, and the magnitude of E used. Although the "unwanted" magnetic field could have been reduced substantially by using a symmetrical dual feed to the plates had it been found necessary.

In order to make the amplitude adjustments of E and H essentially independent it was also necessary to minimize the electric and magnetic coupling between the two field systems. This was accomplished basically by operating each generator in a balanced (push-pull) mode and by physically placing each generator in the neutral plane of the other. When the system was installed at Brooks Air Force Base, there was no observable cross-coupling between the two field generators even when operating at a full kilowatt of RF input power, or when the loop was rotated out of its initial plane of symmetry by any desired angle.

It was pointed out that the RF driving power for each field generator is determined by the associated conductor-, and dielectric-losses, the radiation losses having been minimized by enclosure in a copper-shielded room. The required RF driving power has been found to be roughly proportional to frequency. Water is circulated through the interior of the loop inductor to maintain it at room temperature. This prevents any adverse effect of an increase in the ambient air temperature on the primates during exposure, and stabilizes the loop tuning which otherwise drifts appreciably as the loop heats up. Special tunable networks and balun transformers provide for impedance matching between the field generators and their RF driving sources.

Under the conditions of use the single-turn inductor can generate a fairly "pure" (low-impedance) H-field of up to 100 amperes per meter over the frequency range of 10 to 30 MHz. The parallel-plate line can likewise generate a fairly "pure"

(high-impedance) E-field of up to 10,000 volts per meter over the same frequency range. An RF driving power of up to one kilowatt is required for each field system depending upon frequency and the field level used. The magnitudes of the electric and magnetic fields can be adjusted essentially independently over a wide range, as well as their relative electrical time-phase, and relative spatial orientation in order to simulate various near-field configurations. Previous research in RF biological hazards has been largely limited to the use of plane-wave fields for making clinical studies. This new device will allow researchers to investigate any near-field effects that may occur at high-field levels.

#### 6. ACKNOWLEDGMENT

The author wishes to acknowledge the support provided by the USAF School of Aerospace Medicine at Brooks Air Force Base, Texas, for the work described in this report. Appreciation is also expressed to Dr. James W. Frazer, Air Force Project Officer, for his assistance and encouragement throughout the project, and for his formulation of the specifications on which the EM synthesizer is based.

The assistance of Drs. Howard E. Bussey and David M. Kerns throughout the project is also gratefully acknowledged, and in particular their suggestion regarding the use of multiple in-phase driving sources to reduce the "unwanted" electric field associated with the magnetic-field generator.

## 7. APPENDIX A

### THE ELECTRIC FIELD ASSOCIATED WITH A LOOP INDUCTOR

7.1 Introduction. First, the electric-field distribution associated with a single-turn loop inductor will be evaluated when the loop is fed from a single-source generator operating at a frequency of 30 MHz. It will then be shown how this electric field can be greatly reduced by the expediency of using multiple in-phase driving sources or feeds distributed symmetrically around the loop. A practical method of achieving the effects of the multiple feeds will also be shown. The single-turn inductor used in these tests had the dimensions as previously given, namely, an average diameter,  $d_1$ , of 21 5/8" (0.549 meter), formed from copper tubing having an outside diameter,  $d_2$ , of 1 5/8" (0.0413 meter).

The low-frequency inductance of such a loop is given in microhenries by the following expression [10] which neglects distributed capacitance:

$$L = 0.2\pi d_1 \left[ 2.303 \log_{10} \left[ \frac{8d_1}{d_2} \right] - 2 + \mu\delta \right], \quad (2)$$

where  $d_1$  and  $d_2$  are in meters, and provided  $d_1/d_2 > 5$ . The quantity  $\mu\delta$  represents the internal inductance, which is negligibly small for copper in this frequency range. For the dimensions given, the low-frequency inductance,  $L$ , is approximately 0.921 microhenry neglecting  $\mu\delta$ . The apparent inductance,  $L'$ , increases with frequency due to partial resonance resulting from: (a) the finite size of the loop; (b) its distributed capacitance; and (c) the gap capacitance (assumed to be 5 pF). At a frequency of 30 MHz the apparent inductance was found to be  $L' = 1.36L = 1.25$  microhenries. The apparent inductive reactance is therefore  $X_L' = 2\pi fL' = 236$  ohms.

The maximum value of magnetic field strength,  $H$ , at the center of the loop, specified by the sponsor is 50 amperes per meter (A/m). The relationship between  $H$ , and the driving current,  $I$ , is given by [11]

$$H = \frac{I}{d_1}, \text{ A/m.} \quad (3)$$

7.2 The Single-Source Loop Inductor. An RF driving current of approximately 25 amperes is required, as determined from Equation (3), which results in a driving voltage of 5900 volts at the loop terminals for an operating frequency of 30 MHz. If the loop is driven by a balanced transmission line with a conductor spacing of 0.1 meter (4.0 inches) the electric field strength in the plane of the transmission line will be of the order of 30,000 volts per meter which will probably surprise a lot of people. The electric field strength associated with the single-source loop is proportional to the driving voltage required to force the desired current around the loop. This voltage is in turn essentially proportional to frequency since  $V \approx I X_L$  (neglecting resistance). Therefore, the electric field associated with a given loop will be greatest at the highest operating frequency, namely 30 MHz in this case.

The measured electric-field distribution for the above loop with a current flow of 25 amperes at a frequency of 30 MHz is shown in Figure 14. It can be seen that the electric-field strength is extremely high for this case and varies from 2.3 to 16.0 kilovolts per meter for the positions shown across the diameter of the loop.

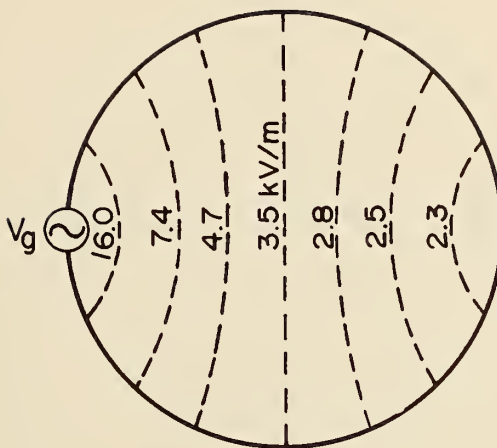


Figure 14. The measured electric-field distribution associated with the single-turn loop inductor having a single driving source at  $f = 30$  MHz.  $I_L = 25$  amp.,  $d_1 = 0.549$  meter,  $V_g = 5900$  volts.

7.3 A Double-Source Loop Inductor. The associated electric-field strength of the previous loop can be appreciably reduced (but not entirely eliminated) by the expediency of using a multiplicity of driving sources properly phased. For example, the driving voltage of the single source in the previous case can be split into two equal parts and fed into the loop at two diametrically opposite points around the loop. The resulting two driving voltages must be in-phase with respect to each other, so that the magnitude of the total driving voltage remains unchanged. The two voltages create electric fields which are spatially 180 degrees out of phase. The resulting electric-field distribution is then as shown in Figure 15.

What happens is that the electric fields of the two sources are, in effect, superposed and subtract everywhere, resulting in a complete cancellation at the center of the loop as shown. The electric field is greatly reduced everywhere except near the second source,  $V_2$  on the right, where it is somewhat greater than before.

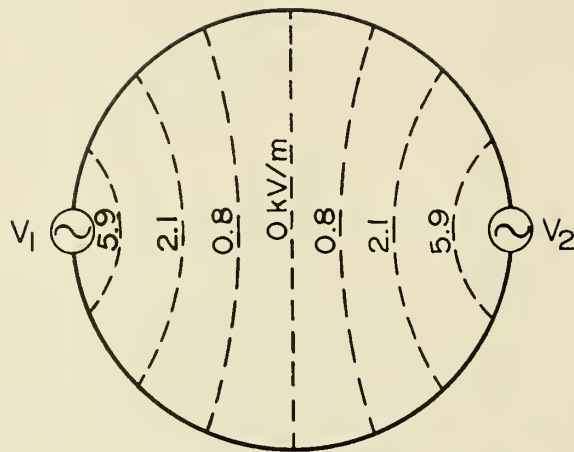


Figure 15. The measured electric-field distribution for the double-source loop inductor.  $V_1 = V_2 = 2425$  volts,  $f = 30$  MHz.

7.4 A Quadruple-Source Loop Inductor. Now, if the total driving voltage is divided into four equal parts, instead of two, and injected every 90 degrees around the loop, such that the four sources are in-phase with respect to each other, the resulting electric-field distribution is as shown in Figure 16.

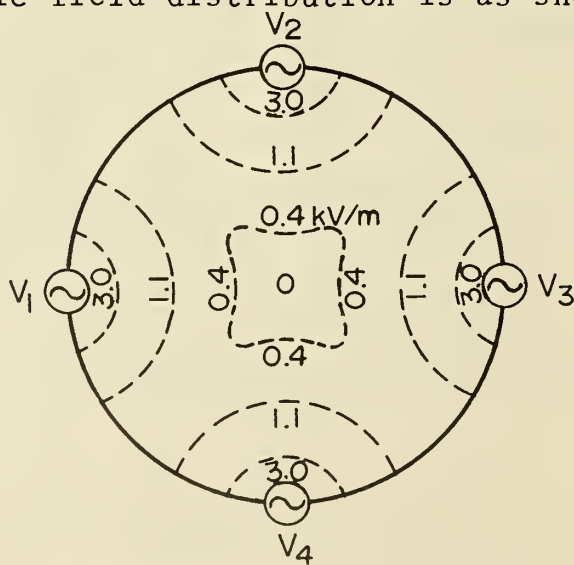


Figure 16. The measured electric-field distribution for the quadruple-source loop inductor.  $V_1 = V_2 = V_3 = V_4 \approx 1150$  volts,  $f = 30$  MHz.

It can be seen that each time the number of sources is doubled the electric field-strength in the vicinity of each source is halved, since each of the driving voltages has been halved. If Figure 16 is compared with Figure 14 it can be seen that the electric-field strength near the center of the loop for the quadruple-source case is only about 1/10 that for the single-source case, so that a substantial reduction in  $E$  in the central region of the loop has been achieved.

### 7.5 A Loop Inductor with a Continuously-Distributed Source.

It soon becomes apparent that four sources is about the upper practical limit, since the electric field in the central portion of the loop will not be appreciably further decreased if the number of sources is further increased as will be shown. The electric-field distribution corresponding to an infinite number of driving sources distributed around the loop can be derived theoretically from one of Maxwell's equations relating  $E$  and  $H$ . For the sinusoidally time-varying, steady-state case, this is [12]

$$\nabla \times \bar{E} = -j\omega\mu\bar{H}. \quad (4)$$

If both sides of equation (4) are integrated over the circular area,  $A = \pi r^2$ , and Stoke's theorem is applied, we obtain

$$\oint_0^{2\pi} \bar{E} \cdot d\ell = -j\omega\mu\bar{H}A. \quad (5)$$

Due to the circular symmetry involved,  $\bar{E} \cdot d\ell$  will be constant around the circular path,  $\ell$ , of radius  $r$  and Equation (5) can be written

$$2\pi rE = -j\omega\mu H(\pi r^2) \quad (6)$$

or

$$E = -j \frac{\omega\mu H r}{2}, \text{ V/m,} \quad (7)$$

where  $E$  is everywhere tangent to the circle of radius  $r$ .  $H$  is normal to the plane of the loop and is essentially constant over the area of the loop except near the loop conductor itself. It can be shown that there is only a second-order increase in  $H$  as  $r$  is increased from 0 to somewhat less than  $r_1$ , the radius of the loop [13]. The magnitude of  $E$  is therefore essentially proportional to  $r$ , at least in the central portion of the loop.

The theoretical electric-field distribution for this case ( $f = 30$  MHz) is shown in Figure 17, corresponding to a loop current of 25 amperes ( $H = 50$  amperes per meter) where the  $E$ -lines are circles as shown. It can be seen that the magnitude

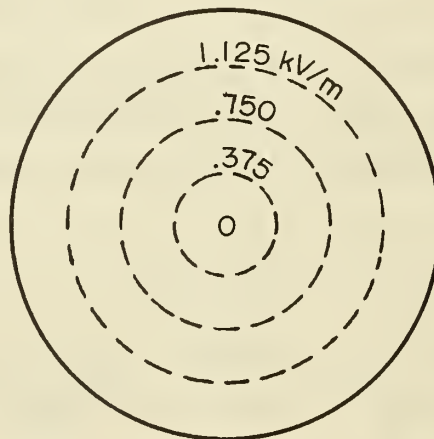


Figure 17. Theoretical electric-field distribution for a loop inductor with a continuously-distributed source ( $H = 50$  amp./m,  $f = 30$  MHz,  $d_1 = 0.549$  m).

of  $E$  in the central portion of the loop with a continuously distributed source is not significantly less than that of the quadruple-source case shown in Figure 16. These values of electric field strength represent the absolute theoretical minimum possible for the value of  $H$  specified; i.e., 50 amperes per meter at 30 MHz.

## 8. APPENDIX B

### METHODS USED TO SIMULATE THE MULTIPLE-SOURCES DRIVING A SINGLE-TURN LOOP INDUCTOR

8.1 Introduction. This section will describe the procedures used to simulate and measure the electric-field distributions of the multiple-source loop inductor given in Appendix A. Advantage was taken of the fact that radial nodal planes exist in these cases, making it necessary to actually provide only a single driving source plus one or more image planes in order to establish the actual electric-field distribution within a single 180 degree or 90 degree sector bounded by the plane/s. The portion of the loop used was formed of two coaxial conductors as will be shown. A gap was cut in the outer conductor at the appropriate place. The RF voltage appearing across this gap served as the loop driving-voltage and so could be positioned as desired around the loop periphery. Sample numerical calculations will be made at a frequency of 30 MHz using conventional transmission-line equations [14].

8.2 The Shielded Half-Loop with a Gap at One End. Figure 18 shows such a 180-degree half-loop, (A), being operated above a ground plane of "infinite" extent. The image of the half-loop is provided in the ground plane. When the full loop is bisected by an image plane, its self impedance is halved. Both the distributed capacitance and the gap capacitance are doubled, but the relative frequency correction, given in Appendix A, Section 7.1, remains unaltered. The equivalent coaxial driving circuit, (B), is terminated in an impedance,  $Z_R = j 118$  ohms, which is half the self-impedance of the full loop ( $X_L' = 236$  ohms) previously given ( $f = 30$  MHz). The line length,  $\ell$ , is half the circumference of the full loop.

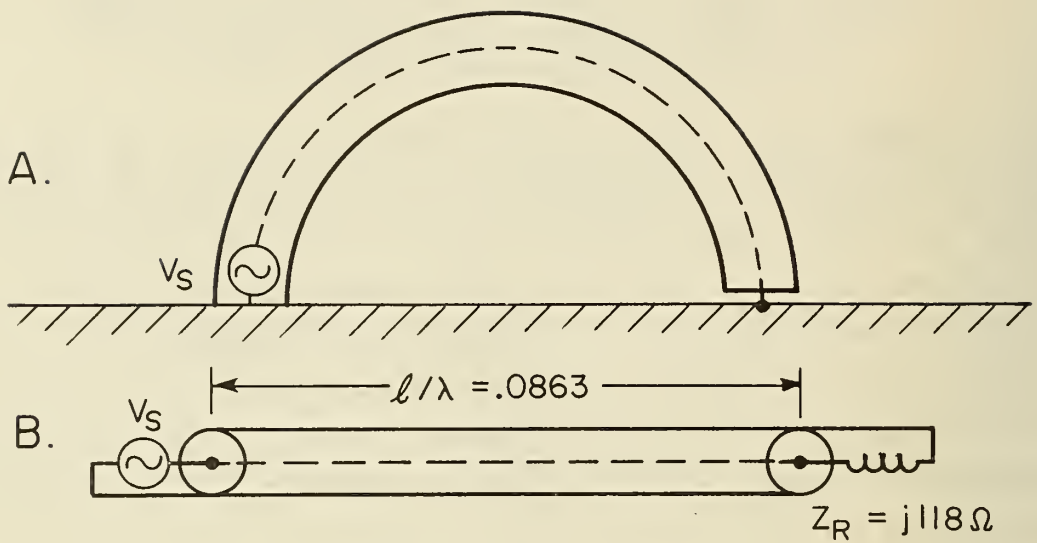


Figure 18. (A) The Shielded 180° Half-Loop with a Gap at One End, situated above an Infinite Image Plane; (B) The Equivalent Coaxial Driving Circuit for Calculating the Various Characteristics of the System using Conventional Transmission Line Equations.  $f = 30$  MHz,  $Z_0 = 41.5$  ohms.

The electric-field distribution above the ground plane will be identical to that of a full 360-degree loop fed with a balanced voltage of double the value. Using a half-loop makes it somewhat easier to set up and measure since only a single-ended driving source and matching network are required. The ground-plane used was an aluminum sheet 48" (122 cm) x 48" (122 cm) x 1/8" (3.18 mm), and the dimensions of the loop were as previously given. The characteristic impedance of the coaxial driving line was 41.5 ohms. Teflon washers, located approximately every 6" (15.2 cm), were used to support the center conductor. These had a minimal effect on the operation of the line owing to the relatively low frequency and completely mismatched conditions used.

The driving-point impedance of the shielded loop was measured at several frequencies over the range from 10 to 30 MHz to verify the equivalent coaxial driving circuit. In all cases the agreement between the measured and calculated values of input impedance was within  $\pm 5$  percent. This means that it is possible to accurately calculate the driving voltage, current, power and the actual gap voltage all for a loop current of 25 amperes at the desired operating frequency using conventional transmission-line equations. Sample calculations of some of these quantities will be made later. The measured electric-field distribution for this case is shown in Figure 14 for the single-source case, except that the missing half has been filled in.

8.3 The Shielded Half-Loop with a Gap at the Center. This half-loop and its equivalent coaxial driving circuit are shown in Figure 19 and, except for the position of the gap and its consequences, has the same general appearance and dimensions as the previous half loop shown in Figure 18. The gap capacitance of 5 pF (Section 7.1) is now across only half of the full loop, so that the frequency correction mentioned in the previous section is now substantially less. This can be seen from the fact that the terminating impedance is now  $Z_R = j 97$  ohms, rather than  $Z_R = j 118$  ohms as for the previous case. In the present case with the gap at the center, the image half-loop in the ground plane provides the effect of a second gap, so that the resultant electric-field distribution above the ground plane is the same as for the double-source loop, shown in Figure 15.

8.4 The Shielded Quarter-Loop with a Gap at the Center. The arrangement of the quarter loop is shown in Figure 20. Here, only one fourth of a full loop is used in conjunction with two orthogonal image planes arranged as shown. The gap capacitance is now across only one quarter of the full loop,

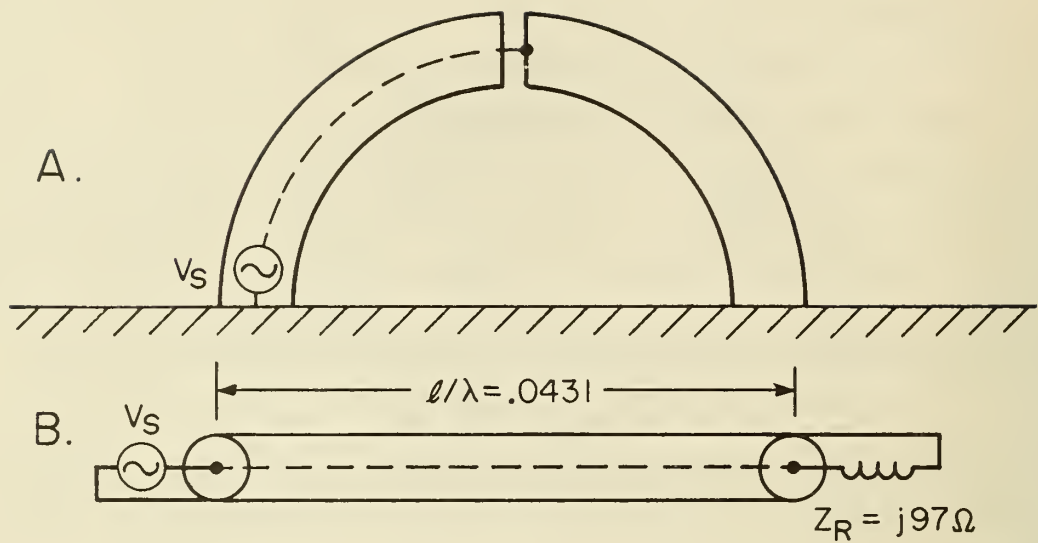


Figure 19. (A) The Shielded 180° Half-Loop with a Gap at the Center, Situated above an Infinite Image Plane; (B) The Equivalent Coaxial Driving Circuit for Calculating the Operating Characteristics.  $f = 30$  MHz,  $Z_0 = 41.5$  ohms.

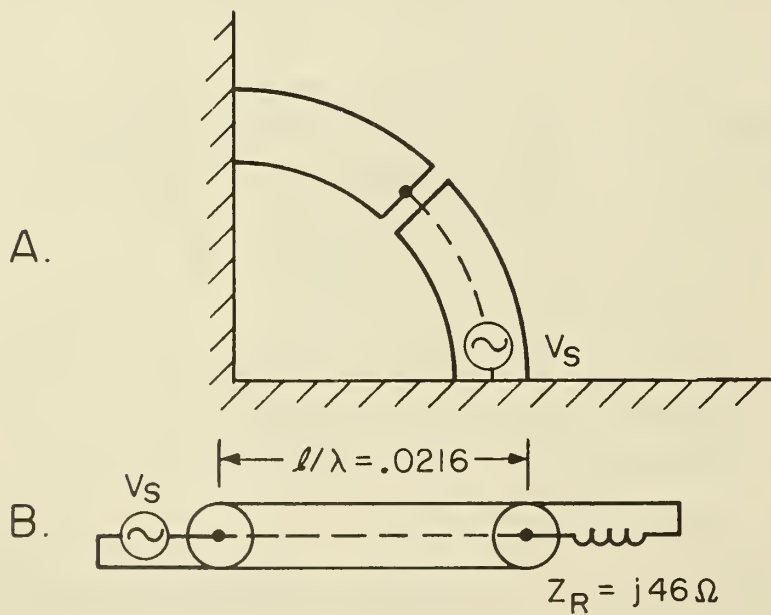


Figure 20. (A) The Shielded 90° Quarter-Loop with a Gap at the Center, Situated between Two Orthogonal Image Planes; (B) The Equivalent Coaxial Driving Circuit for Calculating the Operating Characteristics.  $f = 30$  MHz,  $Z_0 = 41.5$  ohms.

making the frequency correction still less than in the previous cases. The terminating impedance is now  $Z_R = j 46$  ohms, compared to  $Z_R = j 59$  ohms (half of  $Z_R = j 118$  ohms). The missing three quarter-loop segments together with their gaps are in effect provided by the two image planes, so that the resultant electric-field distribution within the 90-degree sector between the planes is the same as for the quadruple-source loop, shown in Figure 16.

It should be clear from Figures 18 to 20 that each time the loop is bisected, the electrical lengths of both the loop and the coaxial driving lines are halved. This raises the self-resonant frequency of the system, and makes it possible for the quadruple-source loop to operate at a much higher frequency than the single-source loop.

**8.5 Calculation of the Loop Characteristics.** The method used to calculate the various voltage, current, and impedance relationships of the loop inductor and its coaxial driving circuit will be outlined in this section using conventional transmission-line equations. Sample numerical calculations will be made for the case of the quarter loop at a frequency of 30 MHz.

The relationship between the sending-end voltage,  $V_S$ , and the receiving-end current,  $I_R$ , of a lossless transmission line of characteristic impedance,  $Z_0$ , when terminated at the receiving end in an impedance,  $Z_R$ , is given by [14]

$$V_S = I_R Z_R \cos \beta \ell + j I_R Z_0 \sin \beta \ell, \quad (8)$$

where  $\ell$  = line length, meters;  $\beta = 2\pi/\lambda$ ; and  $Z_0 = 41.5$  ohms. Substituting the parameters shown in Figure 20, in Equation (8) with  $I_R = 25$  amp., gives

$$V_S = j 25(46 \cos 7.78^\circ + 41.5 \sin 7.78^\circ) = j 1280 \text{ volts.}$$

The gap voltage,  $V_R$ , may be determined from the relationship,

$$V_R = I_R Z_R = j 1150 \text{ volts},$$

which is the loop driving voltage used in Figure 16. The terminating impedance,  $Z_R$ , is the impedance of the quarter loop, as discussed in Section 8.4, where  $Z_R = jX'_L = j 46 \text{ ohms}$  as indicated in Figure 20.

The sending-end current,  $I_S$ , is given by [14]

$$I_S = I_R \cos \beta l + j \frac{I_R Z_R}{Z_0} \sin \beta l \quad (9)$$

$$I_S = 25(\cos 7.78^\circ - \frac{46}{41.5} \sin 7.78^\circ) = 21.02 \text{ amp.}$$

$$Z_S = V_S/I_S = j 1280/21.02 = j 60.89 \text{ ohms.}$$

$Z_S$  represents the driving-point impedance at the sending-end of the coaxial line which is really  $Z_R$  transformed by the transmission line. This is the reactance which is tuned out by each of the vacuum capacitors in Figure 4. In effect, each capacitor tunes its own quarter of the full loop in actual practice.

The RF driving power can also be determined, using the complete, hyperbolic transmission-line equations [14]. This would involve the accurate calculation of the RF resistance of the loop inductor and the four coaxial feed lines [15], and, of course, is more involved than the calculations made above for the lossless case. A preliminary estimate of the required RF driving power can also be obtained, when necessary, from a scaled measurement made at a low-field level.

## 9. REFERENCES

- [1] Jasik, H. (editor), Antenna Engineering Handbook, pp. 6-1 to 6-4 (McGraw-Hill Book Co., Inc., New York, N.Y., 1961).
- [2] Kraus, J.D., Antennas, pp. 155-172 (McGraw-Hill Book Co., Inc., New York, N.Y., 1950).
- [3] Libby, L.L., Special Aspects of Balanced Shielded Loops, Proc. IRE, 34, pp. 641-646 (Sept. 1946).
- [4] Weeks, W.L., Antenna Engineering, pp. 56-61 (McGraw-Hill Book Co., Inc., New York, N.Y., 1968).
- [5] Terman, F.E., Electronic and Radio Engineering, pp. 50-57 (McGraw-Hill Book Co., Inc., New York, N.Y., 1955).
- [6] Sabaroff, S., The Balun "Formalized," IEEE Trans. EMC, Vol. EMC-16, No. 1, pp. 48-50, (Feb. 1974).
- [7] White, D.R.J., EMI Test Instrumentation and Systems, Vol. 4, pp. 4.20-4.24 (Don White Consultants, Germantown, Maryland, 1971).
- [8] Ramo, S., Whinnery, J.R., and Van Duzer, T., Fields and Waves in Communication Electronics, pp. 541-543 (John Wiley & Sons, Inc., New York, N.Y., 1965).
- [9] Jasik, H., op. cit., pp. 20-27 to 20-28.
- [10] Radio Instruments and Measurements, NBS Circular C-74, p. 250, eq. 147 (Jan. 1937).
- [11] Greene, F.M., The Near-Zone Magnetic Field of a Small Circular-Loop Antenna, NBS J. of Res., 71C, No. 4, p. 323, eq. 26 (Oct.-Dec. 1967).
- [12] Ramo, S., Whinnery, J.R., and Van Duzer, T., op. cit., p. 228-238.
- [13] Greene, F.M., loc. cit.
- [14] Guillemin, E.A., Communication Networks, Vol. II, p. 69 (John Wiley & Sons, Inc., New York, N.Y., 1935).
- [15] Wheeler, H.A., Formulas for the Skin Effect, Proc. IRE, 30, pp. 412-424 (Sept. 1942).

U.S. DEPT. OF COMM. BIBLIOGRAPHIC DATA SHEET		1. PUBLICATION OR REPORT NO.  NBS TN-652	2. Gov't Accession No.	3. Recipient's Accession No.
4. TITLE AND SUBTITLE  Development and Construction of an Electromagnetic Near-Field Synthesizer.		5. Publication Date  May 1974		
7. AUTHOR(S) Frank M. Greene		6. Performing Organization Code		
9. PERFORMING ORGANIZATION NAME AND ADDRESS  NATIONAL BUREAU OF STANDARDS DEPARTMENT OF COMMERCE Boulder, Colorado 80302		10. Project/Task/Work Unit No. 2727433		
12. Sponsoring Organization Name and Complete Address (Street, City, State, ZIP)  USAF School of Aerospace Medicine, Brooks Air Force Base, Texas 78235		11. Contract/Grant No. USAF Memorandum of Agree ment, dated 3 Jan. 19		
15. SUPPLEMENTARY NOTES		13. Type of Report & Period Covered Final Report 1/3/72 to 6/30/73		
16. ABSTRACT (A 200-word or less factual summary of most significant information. If document includes a significant bibliography or literature survey, mention it here.)  This publication describes work done by the National Bureau of Standards for the USAF School of Aerospace Medicine at Brooks AF Base involving the development, design, construction and testing of a prototype EM near-field synthesizer. The purpose of the contract was to provide a means of independently generating high-level electric and magnetic near fields in the frequency range 10 to 30 MHz. These fields are to be used in various ratios by the USAFSAM in their EM radiation exposure program for determining the biological effects of hazard-level, non-ionizing EM fields on human beings.		14. Sponsoring Agency Code		
The synthesizer consists of a balanced, parallel-plate strip line to generate the "desired" electric field, and a single-turn quadruple-feed inductor placed parallel to and midway between the plates to generate the "desired" magnetic field. Methods used to reduce the "unwanted" E- and H-field components associated with the above, as well as the methods used to reduce the coupling between the two field systems are discussed. The result is a synthesizer in which the electric- and magnetic-field components can be adjusted essentially independently over wide ranges of magnitude, relative time-phase, and spatial orientation to simulate various near-field configurations.				
Previous research has been largely limited to the use of plane-wave fields for evaluating RF biological hazards. This new device will allow researchers to investigate any near-field effects that may occur at high field levels.				
17. KEY WORDS (six to twelve entries; alphabetical order; capitalize only the first letter of the first key word unless a proper name; separated by semicolons) Electromagnetic-field hazards; electromagnetic-field synthesizer; electromagnetic radiation-exposure testing (non-ionizing); near fields; RF biological hazards.				
18. AVAILABILITY  <input checked="" type="checkbox"/> Unlimited  <input type="checkbox"/> For Official Distribution. Do Not Release to NTIS  <input type="checkbox"/> Order From Sup. of Doc., U.S. Government Printing Office Washington, D.C. 20402, SD Cat. No. C13, 46:652  <input type="checkbox"/> Order From National Technical Information Service (NTIS) Springfield, Virginia 22151		19. SECURITY CLASS (THIS REPORT)  UNCL ASSIFIED	21. NO. OF PAGES  44	
		20. SECURITY CLASS (THIS PAGE)  UNCLASSIFIED	22. Price  \$.50	

# NBS TECHNICAL PUBLICATIONS

## PERIODICALS

**JOURNAL OF RESEARCH** reports National Bureau of Standards research and development in physics, mathematics, and chemistry. Comprehensive scientific papers give complete details of the work, including laboratory data, experimental procedures, and theoretical and mathematical analyses. Illustrated with photographs, drawings, and charts. Includes listings of other NBS papers as issued.

Published in two sections, available separately:

### • Physics and Chemistry (Section A)

Papers of interest primarily to scientists working in these fields. This section covers a broad range of physical and chemical research, with major emphasis on standards of physical measurement, fundamental constants, and properties of matter. Issued six times a year. Annual subscription: Domestic, \$17.00; Foreign, \$21.25.

### • Mathematical Sciences (Section B)

Studies and compilations designed mainly for the mathematician and theoretical physicist. Topics in mathematical statistics, theory of experiment design, numerical analysis, theoretical physics and chemistry, logical design and programming of computers and computer systems. Short numerical tables. Issued quarterly. Annual subscription: Domestic, \$9.00; Foreign, \$11.25.

## DIMENSIONS, NBS

The best single source of information concerning the Bureau's measurement, research, developmental, cooperative, and publication activities, this monthly publication is designed for the layman and also for the industry-oriented individual whose daily work involves intimate contact with science and technology —*for engineers, chemists, physicists, research managers, product-development managers, and company executives*. Annual subscription: Domestic, \$6.50; Foreign, \$8.25.

## NONPERIODICALS

**Applied Mathematics Series.** Mathematical tables, manuals, and studies.

**Building Science Series.** Research results, test methods, and performance criteria of building materials, components, systems, and structures.

**Handbooks.** Recommended codes of engineering and industrial practice (including safety codes) developed in cooperation with interested industries, professional organizations, and regulatory bodies.

**Special Publications.** Proceedings of NBS conferences, bibliographies, annual reports, wall charts, pamphlets, etc.

**Monographs.** Major contributions to the technical literature on various subjects related to the Bureau's scientific and technical activities.

**National Standard Reference Data Series.** NSRDS provides quantitative data on the physical and chemical properties of materials, compiled from the world's literature and critically evaluated.

**Product Standards.** Provide requirements for sizes, types, quality, and methods for testing various industrial products. These standards are developed cooperatively with interested Government and industry groups and provide the basis for common understanding of product characteristics for both buyers and sellers. Their use is voluntary.

**Technical Notes.** This series consists of communications and reports (covering both other-agency and NBS-sponsored work) of limited or transitory interest.

**Federal Information Processing Standards Publications.** This series is the official publication within the Federal Government for information on standards adopted and promulgated under the Public Law 89-306, and Bureau of the Budget Circular A-86 entitled, Standardization of Data Elements and Codes in Data Systems.

**Consumer Information Series.** Practical information, based on NBS research and experience, covering areas of interest to the consumer. Easily understandable language and illustrations provide useful background knowledge for shopping in today's technological marketplace.

## BIBLIOGRAPHIC SUBSCRIPTION SERVICES

The following current-awareness and literature-survey bibliographies are issued periodically by the Bureau:

**Cryogenic Data Center Current Awareness Service** (Publications and Reports of Interest in Cryogenics). A literature survey issued weekly. Annual subscription: Domestic, \$20.00; foreign, \$25.00.

**Liquefied Natural Gas.** A literature survey issued quarterly. Annual subscription: \$20.00.

**Superconducting Devices and Materials.** A literature survey issued quarterly. Annual subscription: \$20.00. Send subscription orders and remittances for the preceding bibliographic services to the U.S. Department of Commerce, National Technical Information Service, Springfield, Va. 22151.

**Electromagnetic Metrology Current Awareness Service** (Abstracts of Selected Articles on Measurement Techniques and Standards of Electromagnetic Quantities from D-C to Millimeter-Wave Frequencies). Issued monthly. Annual subscription: \$100.00 (Special rates for multi-subscriptions). Send subscription order and remittance to the Electromagnetic Metrology Information Center, Electromagnetics Division, National Bureau of Standards, Boulder, Colo. 80302.

Order NBS publications (except Bibliographic Subscription Services) from: Superintendent of Documents, Government Printing Office, Washington, D.C. 20402.

**U.S. DEPARTMENT OF COMMERCE**  
**National Bureau of Standards**  
Washington, D.C. 20234

—  
OFFICIAL BUSINESS

Penalty for Private Use, \$300

POSTAGE AND FEES PAID  
U.S. DEPARTMENT OF COMMERCE  
COM-215

